

# Establishment of the Dorsal–Ventral Axis in *Xenopus* Embryos Coincides with the Dorsal Enrichment of Dishevelled That Is Dependent on Cortical Rotation

Jeffrey R. Miller,\* Brian A. Rowning,\*<sup>‡</sup> Carolyn A. Larabell,<sup>‡</sup> Julia A. Yang-Snyder,\* Rebecca L. Bates,\* and Randall T. Moon\*

\*Howard Hughes Medical Institute, Department of Pharmacology, and Center for Developmental Biology, University of Washington School of Medicine, Seattle, Washington 98195; and <sup>‡</sup>Lawrence Berkeley National Laboratory, University of California at Berkeley, Berkeley, California 94720

**Abstract.** Examination of the subcellular localization of Dishevelled (Dsh) in fertilized *Xenopus* eggs revealed that Dsh is associated with vesicle-like organelles that are enriched on the prospective dorsal side of the embryo after cortical rotation. Dorsal enrichment of Dsh is blocked by UV irradiation of the vegetal pole, a treatment that inhibits development of dorsal cell fates, linking accumulation of Dsh and specification of dorsal cell fates. Investigation of the dynamics of Dsh localization using Dsh tagged with green fluorescent protein (Dsh-GFP) demonstrated that Dsh-GFP associates with small vesicle-like organelles that are directionally transported along the parallel array of microtubules towards the prospective dorsal side of the embryo during cortical rotation. Perturbing the assem-

bly of the microtubule array with D<sub>2</sub>O, a treatment that promotes the random assembly of the array and the dorsalization of embryos, randomizes translocation of Dsh-GFP. Conversely, UV irradiation of the vegetal pole abolishes movement of Dsh-GFP. Finally, we demonstrate that overexpression of Dsh can stabilize  $\beta$ -catenin in *Xenopus*. These data suggest that the directional translocation of Dsh along microtubules during cortical rotation and its subsequent enrichment on the prospective dorsal side of the embryo play a role in locally activating a maternal Wnt pathway responsible for establishing dorsal cell fates in *Xenopus*.

**Key words:** Dishevelled • green fluorescent protein •  $\beta$ -catenin • *Xenopus* • microtubules

**T**HE specification of the dorsal–ventral axis in *Xenopus* is dependent on the translocation of a dorsalizing activity from the vegetal pole to the prospective dorsal side of the embryo during the first cell cycle (reviewed in Harland and Gerhart, 1998; Moon and Kimelman, 1998). The translocation of the dorsalizing activity is dependent on the assembly of a parallel array of subcortical microtubules that appear to act as tracks along which the dorsalizing activity moves (Elinson and Rowning, 1988). Rearing eggs in microtubule stabilizing agents such as D<sub>2</sub>O causes the precocious, random assembly of the microtubule array, the randomized movement of the dorsalizing activity, and the development of radially dorsalized embryos (Scharf et al., 1989; Rowning et al., 1997). Con-

versely, treating eggs with agents that block the assembly of the microtubule array inhibits the movement of the dorsalizing activity, leading to embryos that lack a dorsal axis (Elinson and Rowning, 1988). Although the molecular identity of the dorsalizing activity is unknown, its movement mimics the translocation of endogenous membrane-bound organelles along the microtubule array toward the future dorsal side of the embryo (Rowning et al., 1997). Thus, during cortical rotation the microtubule array appears to act as tracks for the directional transport of a dorsalizing activity, perhaps via its association with membrane-bound organelles, to the prospective dorsal side of the embryo.

Although the molecular nature of the dorsalizing activity is unknown, its movement to the prospective dorsal side is thought to locally stimulate a maternal Wnt signaling pathway that leads to the subsequent activation of dorsal-specific regulatory genes (reviewed in Moon and Kimelman, 1998). The importance of Wnt signaling in regulating the specification of dorsal cell fates in *Xenopus* is well established. Overexpression of various components of

The first two authors contributed equally to this paper.

Address correspondence to Randall T. Moon, Room K536C Health Sciences Building, Campus Box 357750, Department of Pharmacology, University of Washington, Seattle, WA 98195. Tel.: (206) 543-1722. Fax: (206) 616-4230. E-mail: rtmoon@u.washington.edu

the Wnt pathway in ventral cells is sufficient to induce the formation of a complete, secondary dorsal axis (reviewed in Moon and Kimelman, 1998). Conversely, antisense oligonucleotide-mediated depletion of maternal mRNA encoding  $\beta$ -catenin, a component of the Wnt-1/Wingless pathway, results in ventralized embryos demonstrating that  $\beta$ -catenin function is required for the development of dorsal cell fates (Heasman et al., 1994). In unperturbed embryos  $\beta$ -catenin normally accumulates in the cytoplasm and nuclei of dorsal blastomeres during early cleavage stages (Larabell et al., 1997), consistent with localized activation of the Wnt pathway (reviewed in Miller and Moon, 1996; Cadigan and Nusse, 1997). This dorsal enrichment of  $\beta$ -catenin is blocked by ectopic expression of glycogen synthase kinase 3 (GSK-3)<sup>1</sup>, a negative regulator of  $\beta$ -catenin stability. These data have led to the proposal that localized inhibition of GSK-3 on the future dorsal side of the embryo promotes the local accumulation of  $\beta$ -catenin (Yost et al., 1996; Larabell et al., 1997).

How might GSK-3 and  $\beta$ -catenin be regulated? Inactivation of GSK-3 in dorsal cells appears to require the presence of a recently identified protein, GBP, that can bind and suppress GSK-3 activity *in vivo* (Yost et al., 1998). The importance of other upstream components of the Wnt pathway in regulating  $\beta$ -catenin function is unclear. Ectopic expression of a dominant negative form of *Xenopus* Wnt-8 (Hoppler et al., 1996) does not prevent the formation of a dorsal axis. Similarly, dominant negative forms of *Xenopus* Dsh (Sokol, 1996), a cytoplasmic component of the Wnt pathway that functions upstream of  $\beta$ -catenin (Nordermeer et al., 1994), also do not block axis formation. However, these studies represent negative results and therefore do not preclude the possibility that upstream components of the Wnt pathway, including Wnts, Frizzleds, and Dsh, are required for the development of dorsal cell fates.

In this study, we have investigated further the mechanisms responsible for the dorsal activation of the Wnt signaling pathway in *Xenopus* eggs and the subsequent specification of dorsal cell fates in embryos. We demonstrate that Dsh associates with vesicle-like organelles that become enriched on the prospective dorsal side of the egg at the end of the first cell cycle, and this accumulation of Dsh persists through early cleavage stages. This polarized distribution of Dsh is blocked by UV irradiation of the vegetal hemisphere, which blocks dorsal axis formation, providing a link between dorsal enrichment of Dsh and the specification of dorsal cell fates. Moreover, examination of the subcellular distribution of Dsh distribution using a Dsh-GFP fusion protein revealed that during cortical rotation Dsh-GFP translocates along the parallel array of microtubules towards the future dorsal side. These data suggest a model in which microtubule-mediated translocation of Dsh to the future dorsal side of the embryo leads to the localized activation of the Wnt signaling pathway, the accumulation of  $\beta$ -catenin in dorsal blastomeres, and the development of dorsal cell fates in *Xenopus*.

1. *Abbreviations used in this paper:* Dsh, Dishevelled; Dsh-GFP, Dsh tagged with green fluorescent protein; GSK-3, glycogen synthase kinase 3; MR, modified ringers; RFz1, Rat Frizzled-1.

## Materials and Methods

### Constructs

Dsh-GFP is described in Yang-Snyder et al. (1996). GFP-tagged Dsh deletion constructs span the following coordinates (expressed as amino acid position): Dsh $\Delta$ DIX (160–736; a new start methionine was introduced by PCR); Dsh $\Delta$ PDZ (1–267 + 381–736); Dsh $\Delta$ DEP (1–433 + 503–736); and Dsh $\Delta$ COOH (1–588).  $\beta$ -catenin-myc is from Yost et al. (1996).

### Generation and Purification of Anti-*Xenopus* Dsh Antibodies

Full-length *Xenopus* Dsh (Sokol et al., 1995) was cloned in frame with glutathione-S-transferase in the vector pGEXT4T (Pharmacia Biotech). After expression in *E. coli*, Dsh-GST fusion protein was purified on GST-Sepharose beads. Approximately 1 mg of purified protein was injected into New Zealand white rabbits over six separate boosts (R and R Rabbitry). The specificity of the antiserum was confirmed by examining its ability to immunoprecipitate *in vitro* translated Dsh, but not  $\beta$ -catenin (data not shown). To affinity purify anti-Dsh IgG, Dsh-GST was linked to Aminolink Plus beads (Pierce) and IgG was bound and eluted by low pH following the manufacturer's protocols. The eluted IgG was then used for immunolocalization of endogenous Dsh.

### Localization of Dsh in Animal Cap Explants and Embryos

To determine the localization of Dsh and epitope-tagged constructs in *Xenopus* animal cap cells, animal cap explants were fixed for 2 h at room temperature in 4% formaldehyde, 0.1% glutaraldehyde, 100 mM KCl, 3 mM MgCl<sub>2</sub>, 2 mM EGTA, 150 mM sucrose, and 10 mM Hepes (pH 7.6). Explants were then washed in PBS and permeabilized in ice-cold Dent's Fix (80% MeOH and 20% DMSO). Explants were incubated in PBSTB (PBS, 0.1% Triton X-100, and 2% BSA) for 1 h at room temperature to block nonspecific binding. Antibody staining was performed in PBSTB. Anti-mouse Dvl-1 antibodies (kindly provided by K. Willert and R. Nusse, Stanford University, Palo Alto, CA) were used at 1:1,000 dilution and anti-c-myc antibody (9E10 monoclonal supernatant) was used at 1:25 dilution. Alexa568 anti-rabbit and Oregon Green anti-mouse secondary antibodies (Molecular Probes) were used at 1:250 dilution. Images were collected using a laser scanning confocal microscope (Nikon PCM2000 Confocal Microscope System; Nikon Inc.).

For whole-mount confocal immunocytochemistry, embryos were fixed overnight in 4% paraformaldehyde, 0.1% glutaraldehyde, 100 mM KCl, 3 mM MgCl<sub>2</sub>, 150 mM sucrose, and 10 mM Hepes (pH 7.6). Fixed embryos were manually dissected into prospective dorsal and ventral halves using the sperm entry point as a marker of the future ventral side. Blocking of nonspecific binding was carried out in Super Block (Pierce). Embryos were incubated overnight with anti-Dvl-1 antibodies (1:1,000 dilution) or affinity-purified anti-XDsh antibodies (1:100) in Super Block, followed by three washes in Super Block. Embryos were then incubated overnight in Texas red-conjugated anti-rabbit (Molecular Probes) secondary antibodies. Embryos were viewed using a laser scanning confocal microscope (model 1024; Bio-Rad Laboratories).

### Time-Lapse Confocal Microscopy

Oocytes were surgically removed from *Xenopus* females and each oocyte was then injected at the center of the vegetal pole with ~20 nl of synthetic RNA. After injection, oocytes were allowed to translate injected RNA at room temperature for 9–11 h. Oocytes were matured in Modified Ringers (MR; 100 mM NaCl, 1.8 mM KCl, 2 mM CaCl<sub>2</sub>, 1 mM MgCl<sub>2</sub>, 4 mM NaHCO<sub>3</sub>, with 5 mM Hepes, pH 7–7.8). MR at pH 7.0 was used for long-term oocyte maintenance, while MR up to pH 7.8 was used for faster maturation. For storage of oocytes longer than 24 h, BSA was added to the MR to a final concentration of 1 mg/ml. To promote maturation, 1  $\mu$ l of progesterone (stock 10 mg/ml in 100% EtOH) was added to defolliculated oocytes in MR and oocytes were then incubated overnight at 16°C.

After germinal vesicle breakdown, oocytes were pricked in the animal hemisphere with a finely drawn glass needle. After test pricking, the quality of the capping contraction was evaluated: if animal hemisphere pigment contraction was weak or absent, sibling oocytes were allowed to mature longer.

To monitor the movement of organelles and Dsh-GFP particles, images

were captured with a BioRad MRC 1024 laser scanning microscope (BioRad Laboratories). The total field of view that was recorded was  $\sim 75 \times 95 \mu\text{m}$  of the vegetal hemisphere at a focal plane within the cortical shear zone 4–8  $\mu\text{m}$  from the vegetal surface of the egg. Images were collected at 1–3-s intervals and typically, multiple 5-min-long movies were recorded from each activated egg throughout the time period of the first cell cycle. As an indicator of subcortical rotation, Nile red was used to label yolk platelets that move away from the dorsal side at an average velocity of 10  $\mu\text{m}/\text{min}$ .

Confocal movies were analyzed on a Silicon Graphics Indy R5000 workstation running Molecular Dynamics ImageSpace (version 3.2). Particle velocities and translocation angles were calculated using a Microsoft Excel spreadsheet macro, written to process organelle coordinates obtained using ImageSpace (macro available upon request).

Hyperdorsalizing  $\text{D}_2\text{O}$  treatments and microtubule destabilizing nocodazole (50  $\mu\text{g}/\text{ml}$ ) or UV irradiation treatments were carried out on matured activated oocytes as previously described with fertilized eggs (Larabell et al., 1997; Rowning et al., 1997). Treatments and imaging were carried out at equivalent time points in the first cell cycle, by taking note of the dish temperature and time elapsed from the moment of prick activation.

### Western Blot Analyses

To determine the levels of endogenous Dsh in dorsal and ventral blastomeres, embryos were marked dorsally with Nile blue at the 4-cell stage and were dissected into dorsal and ventral halves at the 64–128-cell stage. Embryo halves were lysed on ice in buffer containing 25 mM Hepes, pH 7.7, 150 mM NaCl, 2 mM DTT, 2 mM EDTA, 5  $\mu\text{g}/\text{ml}$  leupeptin, 5  $\mu\text{g}/\text{ml}$  aprotinin, 4 mM PMSF, and 1% digitonin. After incubating for 30 min on ice, cleared lysates were prepared by centrifuging samples for 10 min at 900 rpm and 4°C. Western blots of lysates were probed with anti-mouse Dvl-1 polyclonal antibodies (1:1,000 dilution) or anti- $\alpha$ -fodrin polyclonal antibodies (1:2,000 dilution; Giebelhaus et al., 1987). To confirm the specificity of the anti-mouse Dvl-1 polyclonal antibodies we performed immunoprecipitations of  $^{35}\text{S}$ -labeled proteins from rabbit reticulocyte lysates. These analyses demonstrated that the anti-Dvl-1 antibodies specifically immunoprecipitated wild-type *Xenopus* Dsh, but not Dsh $\Delta\text{COOH}$ -GFP, which lacks the carboxy-terminal epitope used to raise the antibody, or the control proteins Axin-myc and GSK-3-GFP (data not shown).

To examine the effect of overexpression of Dsh on steady state levels of  $\beta$ -catenin, 2-cell embryos were coinjected with RNAs encoding  $\beta$ -catenin-myc and either GFP or Dsh-GFP. Stage 8–9 embryos were homogenized on ice in buffer containing 25 mM Tris (7.5), 150 mM NaCl, 1 mM EDTA, 1 mM EGTA, 0.1% Triton X-100, 5  $\mu\text{g}/\text{ml}$  leupeptin, and 5  $\mu\text{g}/\text{ml}$  aprotinin. Lysates were cleared by centrifugation at 15,000 rpm for 10 min at 4°C. Western blots of lysates were probed with either an anti-*c-myc* antibody (1:50 dilution) or anti- $\alpha$ -fodrin antibodies (1:2,000 dilution).

### Online Supplemental Material

Figure 3, Supplemental Video: Dsh-GFP organelles are shown moving along microtubule tracks towards the prospective dorsal side during cortical rotation. The Dsh-GFP organelles are in green, while the yolk platelets are shown in red. The prospective dorsal side is defined as the side of the egg opposite that prick-activated by a needle. Each movie frame was captured at 1.5-s intervals. See Fig. 3 for static presentation and for analysis of representative data at two selected time points. Videos available at <http://www.jcb.org/cgi/content/full/146/2/427/F3/DC1>

Figure 5, Supplemental Video: Dsh-GFP organelles are shown in prick-activated eggs moving along microtubule tracks that have been randomized by D20. As in the control eggs (see Figure 3, Supplementary Video), Dsh-GFP organelles are shown in green, while yolk platelets are shown in red. See Fig. 5 for static presentation and for analysis of representative data at two selected time points. Videos available at <http://www.jcb.org/cgi/content/full/146/2/427/F5/DC1>

## Results

### Subcellular Localization of Dsh in *Xenopus* Animal Cap Explants

Animal cap explants of *Xenopus* embryos are a useful tissue to analyze the subcellular distribution of signaling proteins (see Miller and Moon, 1997 for example). Therefore,

we analyzed the subcellular distribution of Dsh in animal cap explants as a starting point for the subsequent examination of Dsh localization in early embryos. Blastula stage animal cap explants were stained with antibodies raised against mouse Dvl-1 (kindly provided by K. Willert and R. Nusse), an ortholog of *Xenopus* Dsh, and the subcellular localization of Dsh was determined by laser scanning confocal microscopy. Dsh localized to unidentified vesicle-like intracellular organelles (0.4–1.0- $\mu\text{m}$  diam; arrows in Fig. 1, A and B) and was also detected diffusely throughout the cytoplasm (Fig. 1, A and B). This pattern was specific to Dsh since staining of animal cap explants with secondary antibodies alone produced no detectable staining (data not shown). This subcellular distribution of Dsh is similar to that observed for ectopic Dsh-GFP in animal cap cells (Yang-Snyder et al., 1996; Axelrod et al., 1998) and the localization of Dsh in *Drosophila* embryos and cells (Yanagawa et al., 1995; Axelrod et al., 1996). The nature of these particles remains to be determined, but the apparent association of Dsh with intracellular vesicles in a variety of systems suggests that this localization is important for the signaling function of Dsh.

Expression of specific members of the Frizzled family of Wnt receptors, such as Rat Frizzled-1 (RFz1), has been shown to promote the localization of ectopic GFP-tagged Dsh to the plasma membrane (Yang-Snyder et al., 1996; Axelrod et al., 1998). Therefore, we asked whether expression of RFz1 promotes the localization of endogenous Dsh to the plasma membrane. RNA encoding *c-myc*-tagged RFz1 (500 pg) was injected at the animal pole of 4-cell stage embryos and blastula stage animal cap explants were stained with a combination of anti-Dvl-1 and anti-*c-myc* antibodies. In response to expression of RFz1-myc, Dsh was found in association with the plasma membrane (Fig. 1 C). RFz1-myc also localized to the plasma membrane (Fig. 1 D) in animal cap cells in agreement with the ability of RFz1 to promote the accumulation of Xwnt-8 to the plasma membrane (Yang-Snyder et al., 1996). Taken together, these data establish that (a) endogenous Dsh is localized to vesicle-like organelles of an unknown nature in *Xenopus*, and (b) an excellent correlation exists between the subcellular distribution of endogenous Dsh and ectopic Dsh-GFP in the absence or presence of ectopic RFz1. One may question why endogenous Dsh is localized in the cytoplasm rather than at the plasma membrane given that ectopic RFz1 recruits Dsh to the membrane, and given that endogenous Frizzleds are expressed in animal cap cells. The simplest explanation is Dsh is in equilibrium with respect to binding partners in the cytoplasm versus the membrane and the levels of endogenous Frizzleds are insufficient to push this equilibrium to the membrane whereas overexpression of Frizzleds at nonphysiological levels dramatically shifts this equilibrium to the membrane. These observations set the stage for experiments described below, examining the distribution of endogenous Dsh and ectopic Dsh-GFP during the time the dorsal-ventral axis is specified.

### Dorsal-Ventral Asymmetry in Dsh Localization After Cortical Rotation

We next investigated whether Dsh is asymmetrically local-

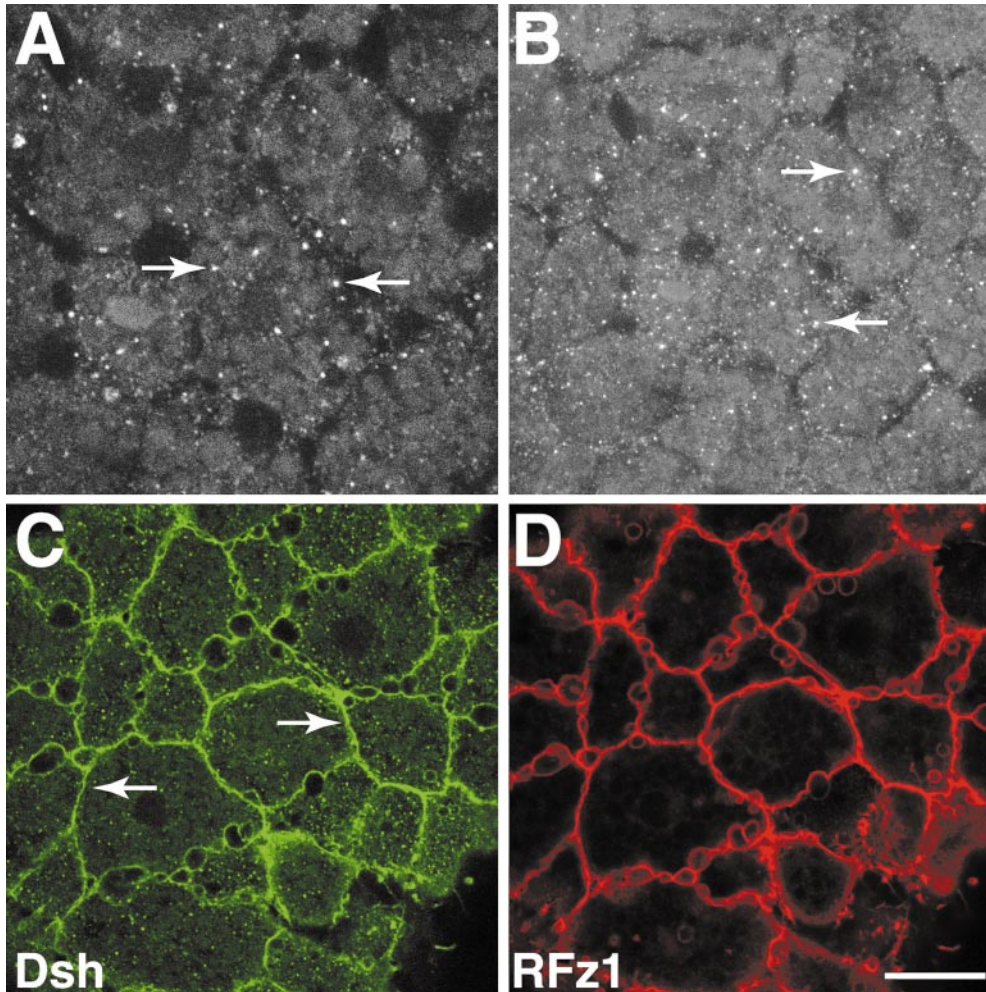


**Figure 1.** Localization of Dsh in animal cap explants and its relocation in response to Frizzled expression. (A and B) Blastula stage animal cap explants were stained with anti-Dvl-1 antibodies and the distribution of Dsh was determined by confocal microscopy. Dsh associates with intracellular vesicle-like organelles (arrows) and is also found diffusely throughout the cytoplasm. (C and D) RNA encoding RFz1-myc was injected into the animal pole of 4-cell stage embryos and the distribution of Dsh (C) and RFz1-myc (D) was determined by confocal microscopy. In response to RFz1-myc expression Dsh accumulated at the plasma membrane (arrows in C). RFz1-myc is also localized to the plasma membrane in animal cap cells. Bar, 20  $\mu$ m.

Downloaded from <http://rupress.org/jcb/article-pdf/146/2/427/12861659901105.pdf> by guest on 08 March 2021

ized along the prospective dorsal-ventral axis in early *Xenopus* embryos. Fertilized eggs were fixed and the localization of Dsh was determined with anti-Dvl-1 and anti-XDsh antibodies. Similar to animal cap explants, Dsh localized to vesicle-like organelles (0.6–1.2- $\mu$ m diam) in the vegetal cortex of fertilized eggs at 0.35–0.4 NT (data not shown, NT; normalized time of the first cell cycle in which 0 = fertilization and 1.0 = first cleavage). To compare the distribution of Dsh along the dorsal-ventral axis, eggs were fixed at 0.7–0.9 NT, manually bisected into dorsal and ventral halves using the sperm entry point as a marker for the future ventral side of the embryo and halves were then stained with anti-Dsh antibodies. Images were then collected from dorsal and ventral equatorial regions at a depth of 4–8  $\mu$ m from the cell surface. Comparison of the staining patterns observed in dorsal and ventral regions using anti-Dvl-1 antibodies ( $N = 10/10$ ) demonstrated that Dsh-associated organelles are more abundant in dorsal equatorial regions (Fig. 2 A) than ventral equatorial regions (Fig. 2 B). Essentially identical results were obtained with affinity-purified anti-*Xenopus* Dsh antibodies (Fig. 2, C and D;  $N = 17/20$ ), confirming the specificity of the staining pattern. Thus, Dsh is enriched in the subcortical cytoplasm on the prospective dorsal side of the embryo after cortical rotation.

The observed dorsal-ventral asymmetry in Dsh distribu-

tion prompted us to ask whether this bias was dependent on cortical rotation. To investigate this question, the distribution of Dsh in prospective dorsal and ventral equatorial regions was examined in embryos in which cortical rotation was blocked by UV irradiation. Vegetal hemispheres of fertilized eggs were UV irradiated at 0.3 NT and the distribution of Dsh was examined by confocal microscopy in treated eggs at 0.7–0.9 NT. UV irradiation of the vegetal hemisphere abolished the dorsal-ventral bias in the distribution of Dsh-associated organelles ( $N = 20/20$ ; data not shown). UV-treated eggs displayed two types of staining patterns. 13 of 20 embryos examined showed Dsh organelles at the vegetal pole and the other seven showed assorted labeling patterns including aggregates of Dsh staining between the vegetal pole and the equator (data not shown). These data demonstrate that Dsh becomes localized to the prospective dorsal side of the embryo in a manner dependent on cortical rotation.

#### ***Dsh-GFP Translocates to the Prospective Dorsal Side During Cortical Rotation***

The asymmetric distribution of endogenous Dsh along the dorsal-ventral axis of fertilized eggs and its sensitivity to UV irradiation prompted us to examine further the relationship between Dsh localization and cortical rotation.

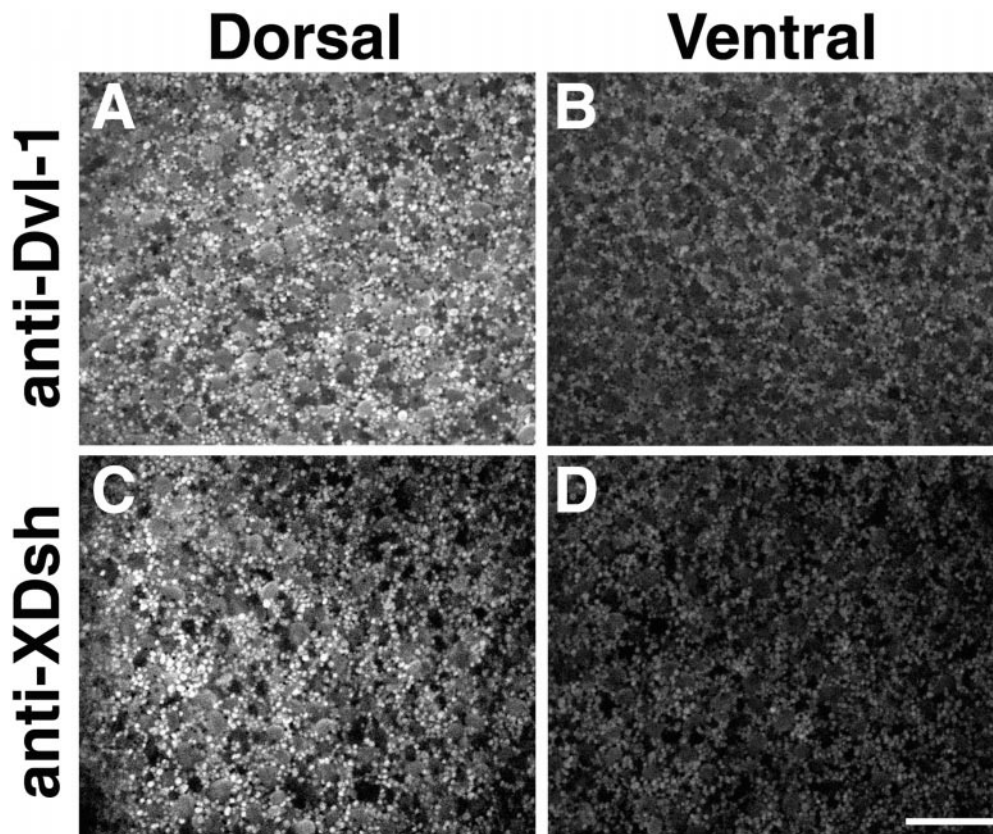


**Figure 2.** Dsh is enriched dorsally after cortical rotation. Eggs at 0.9 of the first cell cycle were fixed, manually dissected into dorsal and ventral halves and then stained with anti-Dvl-1 (A and B) or affinity-purified anti-*Xenopus* Dsh (C and D) antibodies. The distribution of Dsh in dorsal and ventral equatorial zones of the same embryo was then determined by confocal microscopy. After cortical rotation, Dsh localized to vesicle-like organelles similar to that seen in animal cap cells and these organelles were highly enriched in dorsal regions (A and C) relative to ventral regions (B and D). Images shown represent a  $65 \times 65$ - $\mu\text{m}$  region at a depth of 4–8  $\mu\text{m}$  from the cell surface. Bar, 20  $\mu\text{m}$ .

Therefore, we used Dsh-GFP (Yang Snyder et al., 1996) and time-lapse confocal microscopy to investigate the dynamics of Dsh localization during cortical rotation in real time. Dsh-GFP was expressed in oocytes and, after in vitro maturation, the subcellular localization of Dsh-GFP was examined in eggs both before and after prick activation, which initiates cortical rotation. Before activation, Dsh-GFP localized to small vesicle-like organelles (0.3–0.5- $\mu\text{m}$  diam) that are enriched in the vegetal cortex relative to the deeper vegetal cytoplasm (data not shown). Staining of fertilized eggs at 0.35–0.4 NT revealed that endogenous Dsh also associates with vesicle-like organelles at the vegetal pole ( $N = 10/10$ , data not shown). Although the na-

ture of these particles is unclear, they may represent a specific class of membrane bound organelles since the movement of Dsh-GFP along microtubule tracks (see below) mimics the movement of endogenous membrane-bound organelles (Rowning et al., 1997). This localization was specific to wild-type Dsh since several control proteins, including three GFP-tagged deletion mutants of Dsh,  $\beta$ -catenin-GFP, and GFP alone did not show an association with vegetally enriched organelles (Table I).

Time-lapse confocal microscopy was used to examine the localization and dynamics of Dsh-GFP organelles near the vegetal pole of activated eggs during cortical rotation. In the brief period when cortical rotation is starting and array microtubules are polymerizing and becoming co-aligned (Larabell et al., 1996), Dsh-GFP particles exhibit short and initially random saltations. These saltations then become increasingly longer in duration and appear directional as cortical rotation proceeds. In the main period of cortical rotation (0.5–0.8 NT), Dsh-GFP particles move directionally along microtubules toward the future dorsal side of the embryo at an average velocity of 28  $\mu\text{m}/\text{min}$  (Fig. 3, A and B; Table I; see Supplemental Video 1). At time 0 (Fig. 3 A), Dsh-GFP particles (shown in green with representative particles labeled with arrows) and Nile red-labeled yolk platelets (shown in red with a representative yolk platelet labeled with Y) are seen in the vegetal shear zone. After 15 s (Fig. 3 B), Dsh-GFP particles showed a marked displacement toward the right side of the field of view while the yolk platelets showed a slight displacement in the opposite direction. The movements of selected Dsh-GFP particles are summarized in Fig. 3 C.

**Table I.** The Effects of Mutations in Dsh-GFP

RNA	Particle in vegetal shear zone	Diameter	Average velocity during rotation
		$\mu\text{m}$	$\mu\text{m}/\text{min}$
Dsh-GFP	Yes	0.3–0.5	28 (18–24)*
Dsh $\Delta$ DIX-GFP	No	NA	NA
Dsh $\Delta$ PDZ-GFP	No	NA	NA
Dsh $\Delta$ DEP-GFP	No	NA	NA
Dsh $\Delta$ COOH-GFP	Yes	0.3–0.5	29.5 (19–40)*
$\beta$ -Catenin-GFP	No <sup>‡</sup>	(7–10)	NA
GFP	No <sup>§</sup>	NA	NA

\*Velocity was measured relative to the immobilized cortex.

<sup>‡</sup>Not at vegetal periphery, though rarely in (or associated) with a few large aggregates of 7–10- $\mu\text{m}$ -diam at the equator.

<sup>§</sup>The GFP control RNA resulted in a general diffuse fluorescent signal in oocytes. In contrast, a “particle” is defined here as any object that registered in confocal imaging as a discrete persistent size = 0.17  $\mu\text{m}$  (1 pixel at 63 $\times$ ).

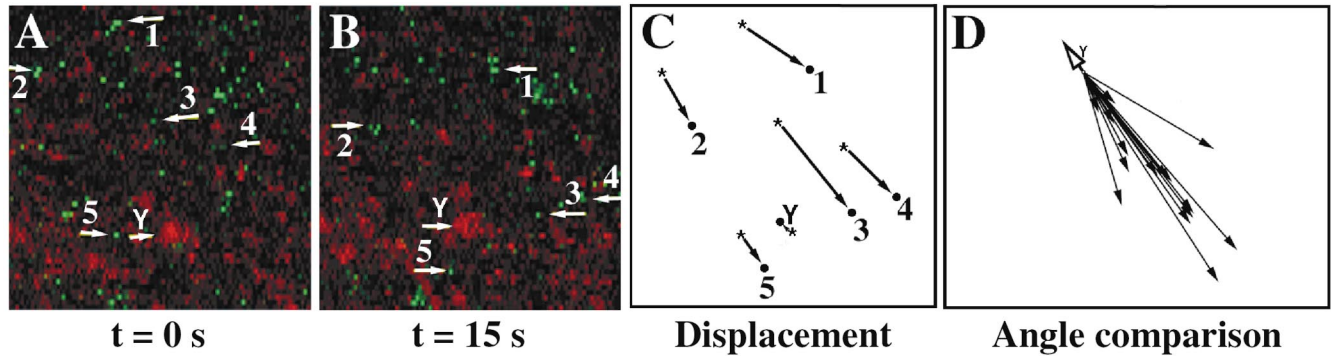


**Figure 3.** Dsh-GFP moves along microtubule tracks to the prospective dorsal side during cortical rotation. (A) Vegetal pole of an egg during the main period of cortical rotation at time 0. (B) Same egg as in A, after 15 s. White arrows point to Dsh-GFP particles whose motion was tracked successively through confocal time-lapse movie frames captured at 1.5-s intervals for at least 15 s. See Video 1 for an example (available at <http://www.jcb.org/cgi/content/full/146/2/427/F3/DC1>). As an indication of the subcortical rotation (a global displacement of core yolk platelets), a white arrow labeled with a Y tracks the motion of a representative subcortical yolk platelet. The field of view shown for all panels is  $35 \times 35 \mu\text{m}$  at a focal plane viewing into subcortical rotation shear zone, 4–8  $\mu\text{m}$  in from the egg's vegetal surface. The total field of view that was recorded was broader,  $\sim 75 \times 95 \mu\text{m}$  of the vegetal hemisphere region. (C) Summary of the displacement of representative Dsh-GFP particles from A and B. (D) Displacement vectors of representative Dsh-GFP particles plotted from a common origin ( $t = 26$  s). The open arrowhead (Y) shows the movement of the egg's yolky core. Dsh-GFP particles move uniformly in the opposite direction from that of the yolk platelets. Since yolk platelets move towards the ventral side these data demonstrate that Dsh-GFP translocates towards the dorsal side of the embryo.

The direction of movement of Dsh-GFP particles in the vegetal shear zone was compared with that of yolk platelets in the same region by plotting the displacement vector for representative Dsh-GFP particles and yolk platelets from a common origin (Fig. 3 D). The orientation of Dsh-GFP saltations was also plotted relative to the direction of subcortical rotation (Fig. 4, A and B). These analyses clearly demonstrate that Dsh-GFP particles are uniformly transported in the opposite direction from yolk platelets, toward the prospective dorsal side of the embryo.

We then examined the effects of treatments that perturb the assembly of the parallel microtubule array on the di-

rectional transport of Dsh-GFP organelles. Treatment of eggs with inhibitors of microtubule polymerization such as UV irradiation or 50  $\mu\text{g/ml}$  nocodazole prevents the dorsal transport of endogenous vesicles during cortical rotation (Rowning et al., 1997) and inhibits the development of dorsal cell fates (Elinson and Rowning, 1988). These treatments also abolished the directional movement of Dsh-GFP organelles (data not shown). In treated eggs, Dsh-GFP particles did not display sustained vectorial translocation and only showed Brownian motion demonstrating that the directional transport of Dsh-GFP requires the assembly of the parallel microtubule array.

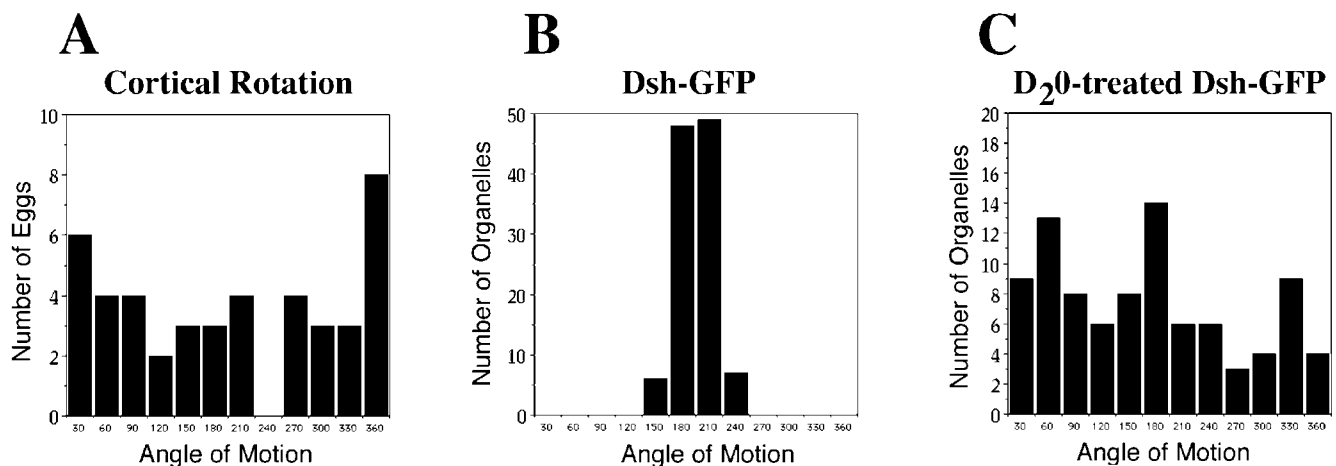


**Figure 4.** Quantitative analysis of Dsh-GFP in normal and microtubule-disrupted eggs. (A) Cortical rotation: this plot shows the angles of subcortical rotation for 44 matured and prick-activated oocytes observed in these experiments, relative to an arbitrary stable reference point on the viewing dish platform that oocytes were placed into for confocal imaging. As expected, the rotation angles were random with respect to this arbitrary reference point. (B) Dsh-GFP. 12 oocytes from 3 female frogs and 110 GFP-tagged organelle saltations were observed. The average orientation of Dsh-GFP saltations was  $180.6^\circ$ , relative to subcortical rotation displacement being at  $0^\circ$ . The range of displacement angles was from  $135.1^\circ$  to  $223.5^\circ$ . Thus displacements tended to occur in a direction  $180^\circ \pm 46^\circ$ , approximately opposite the direction of subcortical rotation. (C) D<sub>2</sub>O-treated Dsh-GFP. 10 oocytes from 3 female frogs were analyzed. The orientation of Dsh-GFP saltations were random relative to subcortical displacement.

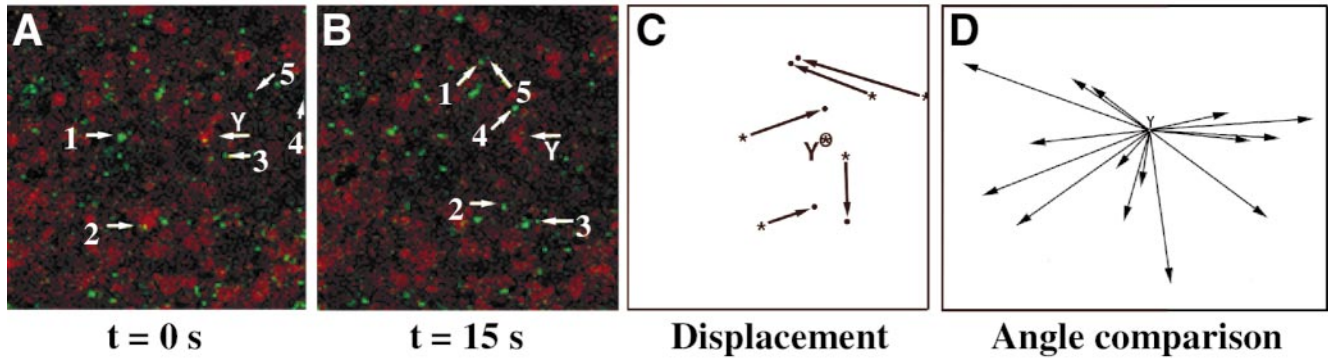


**Figure 5.** Translocation of Dsh-GFP is randomized in  $D_2O$ -treated eggs. (A) Egg treated with  $D_2O$  at time 0. (B) Same egg as in A, after 15 s. White arrows point to Dsh-GFP particles whose motion was tracked successively through confocal time-lapse movie frames captured at 1.5-s intervals for at least 15 s. See Video 2 for an example (available at <http://www.jcb.org/cgi/content/full/146/2/427/F5/DC1>). (C) Summary of the displacement of representative Dsh-GFP particles from A and B. (D) Displacement vectors of Dsh-GFP particles plotted from a common origin demonstrating that  $D_2O$  treatment results in the random translocation of Dsh-GFP particles ( $t = 26$  s).

Treatment of fertilized eggs with 70%  $D_2O$  causes dorsalization of embryos and reduces the extent of cortical rotation by causing the precocious formation of a random meshwork of microtubules in the vegetal cortex (Scharf et al., 1989).  $D_2O$  treatment also randomizes the movement of endogenous organelles in the vegetal shear zone suggesting that the dorsalizing effects of  $D_2O$  may be due to the random transport of dorsalizing factors from the vegetal pole to the entire equatorial region (Rowning et al., 1997). In  $D_2O$ -treated eggs, the average velocity of Dsh-GFP particles during rotation was  $24.33 \mu\text{m}/\text{min}$ , similar to the velocities of Dsh-GFP particles in untreated eggs. In addition, Dsh-GFP particles displayed vectorial saltations similar in duration to that seen in untreated eggs. However, Dsh-GFP particles did not move uniformly towards the dorsal side and instead moved randomly in all directions (Fig. 5, A–D; see Supplemental Video 2). The movement of representative Dsh-GFP particles is depicted in Fig. 5, A and B (Dsh-GFP particles are shown in green and are marked with white arrows, the time between A and B is 15 s) and is summarized in Fig. 5 C. Plots of the vector displacement angles for selected Dsh-GFP particles clearly show that their movement is randomized after  $D_2O$  treatment (Figs. 4 C and 5 D). Together, these data suggest that the directional movement of both ectopic Dsh-GFP and endogenous Dsh are dependent upon the parallel array of microtubules.

### Dsh Is Enriched Dorsally in Cleavage Stage Embryos

The observed dorsal bias in Dsh staining may represent a difference in a specific vesicle-associated pool of Dsh or a difference in the overall levels of Dsh in dorsal and ventral regions. To differentiate between these possibilities, Western blots of protein lysates prepared from dorsal and ventral regions of 64–128-cell stage embryos were probed with anti-Dvl-1 antibodies. These analyses demonstrated that Dsh is enriched in dorsal halves relative to ventral halves of cleavage stage embryos (Fig. 6 A). Levels of Dsh in dorsal halves were found to be  $\sim 2.4$ -fold greater than levels seen in ventral halves after normalization to levels of  $\alpha$ -fodrin, a control protein that does not show a dorsal-ventral

asymmetry (fold difference represents an average from four independent experiments; normalized D/V difference for the blot shown in Fig. 6 A = 1.44). In both dorsal and ventral lysates, Dsh appeared as a doublet with the higher mobility form being present at greater levels than the lower mobility form. These distinct forms of Dsh may represent different phosphorylation variants similar to that observed in *Drosophila* (Yanagawa et al., 1995) although the significance of this observation remains unclear.

We then examined whether the asymmetry in the levels of Dsh in cleavage stage embryos is dependent on cortical rotation. Fertilized eggs were UV irradiated to block cortical rotation and Western blot analysis was used to determine the levels of Dsh in lysates prepared from prospec-

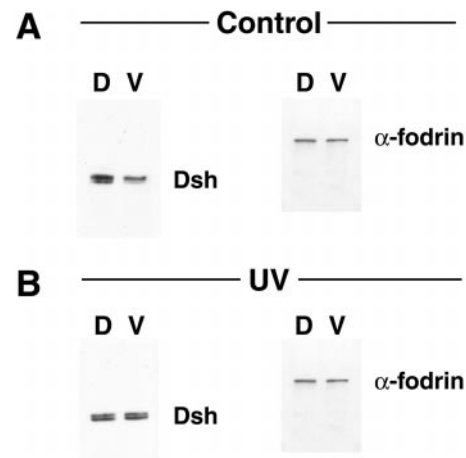


**Figure 6.** Endogenous Dsh is present at higher levels in dorsal blastomeres relative to ventral blastomeres and this asymmetry is dependent on cortical rotation. Lysates from dorsal and ventral regions of control (A) and UV-irradiated (B) 64–128-cell stage embryos were immunoblotted with anti-Dvl-1 antibodies. (A) In control embryos, steady state levels of Dsh are higher in dorsal regions relative to ventral regions. (B) After UV irradiation, this asymmetry is abolished. Lysates were also probed with anti- $\alpha$ -fodrin antibodies to control for total protein content and gel loading (lower panels).  $\alpha$ -Fodrin levels do not exhibit dorsal-ventral differences in either control or UV-irradiated embryos.

tive dorsal and ventral regions of treated 64–128-cell stage embryos. Although UV irradiation prevents dorsal development, embryos still display pigment differences at the 4-cell stage and this asymmetry was used to determine the prospective dorsal–ventral axis. Inhibition of cortical rotation by UV irradiation eliminated the dorsal–ventral difference in the levels of Dsh (Fig. 6 B). After normalization to levels of  $\alpha$ -fodrin, levels of Dsh in dorsal lysates were found to be  $\sim 0.85$ -fold less than that observed in ventral lysates in UV-treated embryos (fold difference represents an average from two experiments). In addition, the relative levels of the two putative phosphorylation forms of Dsh also changed after UV treatment. In both dorsal and ventral lysates of UV-treated embryos, the lower mobility form of Dsh is present at greater levels than the higher mobility form. Together, these data confirm the confocal microscopy analyses showing that Dsh is enriched in dorsal regions of the embryo and that this asymmetry is dependent on cortical rotation.

### Overexpression of Dsh Stabilizes $\beta$ -catenin

The observations that the dorsal enrichment of Dsh and  $\beta$ -catenin (Larabell et al., 1997) is dependent on cortical rotation, and that Dsh functions upstream of  $\beta$ -catenin in the Wnt pathway (Nordermeer et al., 1994), suggest that the dorsal accumulation of Dsh plays a role in promoting the stabilization of  $\beta$ -catenin in dorsal cells. Since this hypothesis has not been directly tested in *Xenopus*, we asked whether overexpression of Dsh can stabilize ectopic  $\beta$ -catenin in *Xenopus* embryos. Ectopic  $\beta$ -catenin was analyzed rather than endogenous  $\beta$ -catenin to monitor the stability of newly synthesized  $\beta$ -catenin and to avoid the large, stable pool of  $\beta$ -catenin present at the plasma membrane in association with cadherins. RNA encoding *c-myc*-tagged  $\beta$ -catenin ( $\beta$ -catenin-myc) was coinjected with either a control RNA (GFP) or Dsh-GFP RNA and the levels of  $\beta$ -catenin-myc in embryo lysates was determined by immunoblotting with anti-*c-myc* antibodies. Overexpression of Dsh-GFP resulted in a marked increase in the steady state levels of  $\beta$ -catenin-myc relative to levels seen in GFP-injected control lysates (Fig. 7). As a control, identical samples were probed with anti- $\alpha$ -fodrin antibodies. Overexpression of Dsh did not affect the levels of  $\alpha$ -fodrin. These data demonstrate that Dsh can regulate the steady state levels of  $\beta$ -catenin in *Xenopus* and that an increase in levels of Dsh is sufficient to stabilize  $\beta$ -catenin.

### Discussion

Current models support the initial hypothesis (McMahon and Moon, 1989) that the localized activation of a maternal Wnt pathway promotes the specification of dorsal cell fates in *Xenopus* (reviewed by Moon and Kimelman, 1998). Specifically,  $\beta$ -catenin is required for dorsal development (Heasman et al., 1994) and it accumulates in dorsal cells in a manner consistent with a role in regulating dorsal cell fate specification (Larabell et al., 1997). This enrichment of  $\beta$ -catenin in dorsal cells is thought to require the local inhibition of GSK-3 (Yost et al., 1996). Despite identification of GBP, a GSK-3-binding protein that is required for development of dorsal cell fates (Yost et al.,

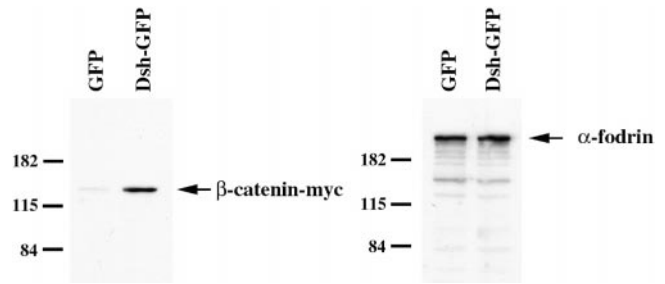


**Figure 7.** Overexpression of Dsh stabilizes  $\beta$ -catenin. Immunoblots of lysates prepared from embryos injected with  $\beta$ -catenin-myc RNA (25 pg) in combination with either GFP RNA (1 ng) or Dsh-GFP RNA (1 ng) reveal that overexpression of Dsh-GFP increases the stability of  $\beta$ -catenin. Lysates were also immunoblotted with anti- $\alpha$ -fodrin antibodies to control for total protein content and gel loading.

1998), to date no studies have demonstrated an asymmetry in localization or function of any component of the Wnt pathway other than  $\beta$ -catenin. Therefore, it has been unclear how the dorsal–ventral asymmetry in GSK-3 activity and  $\beta$ -catenin levels are regulated. Here we address the unresolved issue of whether Dsh plays a role in regulating the localized activation of a maternal Wnt signaling pathway that promotes stabilization of  $\beta$ -catenin and specification of dorsal cell fates in *Xenopus*. We find that Dsh accumulates on the prospective dorsal side of the egg after cortical rotation and this dorsal enrichment appears to be dependent upon the microtubule-mediated directional transport of Dsh. These results strongly implicate Dsh as an important regulator of dorsal–ventral axis formation and provide the first mechanistic link between cortical rotation and the asymmetric activation of a maternal Wnt pathway responsible for regulating the development of dorsal cell fates in *Xenopus*.

### Dorsal Enrichment of Dsh and the Specification of Dorsal Cell Fates

The translocation of Dsh-GFP along the parallel array of subcortical microtubules towards the prospective dorsal side, and the dorsal enrichment of endogenous Dsh coincides with the ability of transplanted cytoplasm to induce the development of dorsal cell fates in host embryos (reviewed in Moon and Kimelman, 1998). Thus, the dynamics of Dsh distribution in early embryos coincides with the localization of the endogenous dorsalizing activity, consistent with the possibility that Dsh plays a role in regulating the specification of the dorsal–ventral axis in *Xenopus*. Importantly, we report here that treatments that perturb dorsal development also affect the distribution of Dsh. UV irradiation of the vegetal hemisphere of fertilized eggs, a treatment that blocks cortical rotation and inhibits dorsal development, prevents the directed movement of Dsh-GFP and the dorsal enrichment of Dsh monitored by confocal microscopy and by Western blot analysis. Conversely, treatment of eggs with  $D_2O$ , which causes hyperdorsalization, results in the random transport of Dsh-GFP suggesting that the movement of Dsh from the vegetal pole to all regions of the equatorial zone promotes the de-



velopment of dorsal cell fates throughout the marginal zone.

The dorsal enrichment of Dsh is also significant because it represents the earliest dorsal–ventral asymmetry in a signaling molecule, and is therefore the best candidate for regulating the localized accumulation of  $\beta$ -catenin on the prospective dorsal side at the end of the first cell cycle (Rowning et al., 1997). In addition, the dorsal enrichment of Dsh persists through early cleavage divisions in agreement with the observed stabilization of  $\beta$ -catenin in dorsal blastomeres of cleavage and blastula stage embryos (Larabell et al., 1997). Taken together with our finding that overexpression of Dsh promotes the stabilization of  $\beta$ -catenin, we propose that the dorsal enrichment of Dsh regulates the establishment of a free, signaling pool of  $\beta$ -catenin on the dorsal side of the embryo. Although the mechanism by which Dsh leads to the stabilization of  $\beta$ -catenin is unclear it may involve direct interactions between Dsh and downstream components of the Wnt pathway. Consistent with this idea, Dsh can form a complex with Axin (Zeng et al., 1997), a negative regulator of  $\beta$ -catenin stability (Yang-Snyder, J.A., J.R. Miller, and R.T. Moon, unpublished observations).

The mechanism by which Dsh becomes enriched on the prospective dorsal side of the embryo appears to involve the directed transport of Dsh along the subcortical microtubule array from the vegetal pole to the future dorsal side during cortical rotation. This idea is supported by the following observations: (a) Dsh-GFP is translocated along the subcortical microtubule array during cortical rotation. (b) Endogenous Dsh accumulates in the dorsal subcortical cytoplasm at a depth 4–8  $\mu$ m from the cell surface in agreement with the location of the subcortical microtubule array (Larabell et al., 1996; Rowning et al., 1997). (c) UV irradiation of the vegetal hemispheres of fertilized eggs prevents cortical rotation and both the directional transport of Dsh-GFP particles and the dorsal accumulation of endogenous Dsh. (d) D<sub>2</sub>O treatment randomizes the microtubule array and also randomizes the movement of Dsh-GFP. (e) The velocities and directional movement of Dsh-GFP particles are sufficient to account for the translocation of a pool of Dsh from the vegetal pole to the dorsal equatorial region during rotation. In addition, the velocities of Dsh-GFP movement are consistent with microtubule-mediated transport. (f) The size and velocities of Dsh-GFP particles are comparable to that of endogenous vegetal vesicles, which are also transported along the microtubule array towards the dorsal side during cortical rotation (Rowning, et al. 1997). This suggests that Dsh may associate with a specific class of vesicles that is transported dorsally during cortical rotation.

Dsh does not possess protein domains typically found in molecular motors, indicating that Dsh is likely transported through its direct or indirect association with microtubule-based motors. These motors may be members of the kinesin family of microtubule-based motors because the plus end-directed movements and velocities of Dsh-GFP particles during cortical rotation are characteristic of transport by kinesin-like motors. Based on these observations, we propose that Dsh, through its association with a distinct class of vesicles, is transported via a kinesin-like motor along the subcortical microtubule array and this move-

ment contributes to the enrichment of Dsh on the prospective dorsal side of the embryo. Furthermore, the translocation of Dsh-GFP particles along microtubule tracks raises the possibility that microtubule-mediated transport of Dsh may represent a general mechanism in other cell types for regulating the subcellular localization of Dsh.

### ***A Revised Model of Dorsal–Ventral Axis Specification in *Xenopus****

Based on previous studies and the data presented in this report, we propose the following model to explain the specification of dorsal cell fates in *Xenopus* (Fig. 8). Before fertilization, Dsh is associated with a specific class of membrane-bound organelles localized to the vegetal cortical region. This pool of Dsh may be unique not only in its localization but also in its associations with other, unidentified proteins. After fertilization, the site of sperm entry biases the direction of cortical rotation and the orientation of the vegetal subcortical microtubule array. Using this microtubule array, Dsh is actively transported towards the prospective dorsal side via a microtubule-based motor system with which Dsh directly or indirectly interacts. This movement may lead to localized function of Dsh through any combination of the following mechanisms: through an increase in levels of Dsh, through an increase in a post-translationally modified form (i.e., phosphorylated) of Dsh, through an increase in a specific complexed form of Dsh, or through an increase in the levels of Dsh in a discrete sub-compartment of dorsal cells. With respect to the latter possibility, cytoplasmic transfer experiments have demonstrated that the dorsalizing activity is highly enriched in the cortical cytoplasm of eggs and in the dorsal cortical cytoplasm after cortical rotation, where it remains through at least the 16-cell stage (Holowacz and Elinson, 1993; Kageura 1997). In addition,  $\beta$ -catenin accumulates to higher levels in the cortical cytoplasm relative to deep cytoplasm of dorsal cells during cleavage stages (Larabell et al., 1997). Since we observe that Dsh is also enriched in the cortical cytoplasm after cortical rotation it is in the appropriate location at the necessary time to promote the observed dorsal accumulation of  $\beta$ -catenin (Larabell et al., 1997).

After cortical rotation, we predict that Dsh functions either directly or indirectly to downregulate the phosphorylation of  $\beta$ -catenin by GSK-3. This activity of Dsh may involve interactions with GBP, a recently described GSK-3-binding protein that is required for the establishment of the dorsal–ventral axis (Yost et al., 1998). Inhibition of GSK-3-dependent  $\beta$ -catenin phosphorylation would result in the posttranslational stabilization of  $\beta$ -catenin and the formation of a free, signaling pool of  $\beta$ -catenin, as previously described (Yost et al., 1996; Aberle et al., 1997; Orford et al., 1997). This signaling pool of  $\beta$ -catenin accumulates in the nucleus (Schneider et al., 1996; Larabell et al., 1997) where, in combination with XTcf-3 (Molenaar et al., 1996), it positively regulates the transcription of *siamois*, *twin*, and *Xnr-3* in dorsal cells (Brannon et al. 1997; Laurent et al., 1997; McKendry et al., 1997). On the ventral side where levels of nuclear  $\beta$ -catenin are low, XTcf-3 works as a transcriptional repressor, perhaps through the activity of Groucho-related proteins (Brannon et al., 1997; Roose et al., 1998) or CtBP (Brannon et al., 1999), to sup-

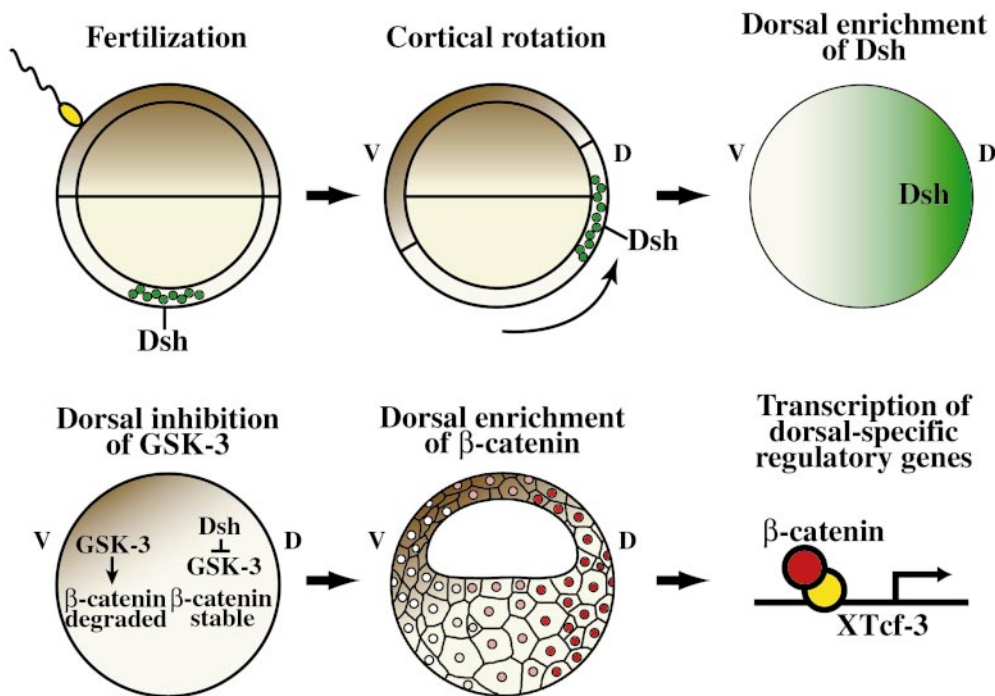


**Figure 8.** Model of the mechanism of localized Wnt pathway activation during dorsal-ventral axis specification in *Xenopus*. Dsh associates with a specific class of vesicles at the vegetal pole and these vesicles are transported dorsally along the subcortical microtubule array during cortical rotation. This translocation contributes to the asymmetric distribution of Dsh along the dorsal-ventral axis and the localized activation of a maternal Wnt signaling pathway. Activation of Wnt signaling leads to the down-regulation of GSK-3 activity thereby promoting the stabilization of  $\beta$ -catenin.  $\beta$ -catenin then accumulates in dorsal nuclei where in combination with XTcf-3 it activates transcription of dorsal-specific regulatory genes. See text for details.

press transcription of dorsal specific regulatory genes. Although this model (Fig. 8) predicts that the molecular mechanism responsible for stabilizing  $\beta$ -catenin in dorsal cells involves only the cytoplasmic components of the Wnt signaling pathway, it remains possible that an endogenous Wnt and/or Frizzled also plays a role in the development of dorsal cell fates.

Is it possible to reconcile this model with the prior evidence that a putative dominant negative version of Dsh does not block formation of the endogenous axis (Sokol, 1996)? We think that this result does not preclude our model based on the following evidence. First, in that study, RNA encoding dominant negative Dsh was injected into fertilized eggs, rather than into oocytes which were then matured and implanted into surrogate hosts to experimentally evaluate the consequences on axial development. Since we propose that a maternally provided pool of Dsh is actively transported to the dorsal side during the first hour after fertilization, levels of the dominant negative Dsh synthesized from injected RNA may have been insufficient to interfere with the function of endogenous Dsh in these experiments. Second, endogenous Dsh may be present in a complex that is unaffected by the expression of ectopic Dsh. Along these lines, we have observed that Dsh can form homodimers in a yeast two-hybrid assay (Cheyette, B., and R.T. Moon, unpublished observations) suggesting that Dsh may form homodimers in vivo. Third, we have shown that a mutant form of Dsh, Dsh $\Delta$ PDZ-GFP, which is similar to the dominant negative Dsh described by Sokol (1996), does not associate with small particles near the vegetal pole. As a result the mutant Dsh is not transported along the microtubule array during cortical rotation suggesting that the dominant negative Dsh

may not localize to sites in the cell necessary to block the function of endogenous Dsh.

To unequivocally demonstrate that Dsh plays a role in regulating the specification of dorsal cell fates in *Xenopus*, it is necessary to examine the effect of removing Dsh function on dorsal development. Since *Xenopus* is not amenable to traditional genetic manipulations, loss-of-function experiments have used antisense oligonucleotide-mediated depletion of maternal mRNA (see for example Heasman et al., 1994). Antisense depletion studies of Dsh RNA have so far reduced but not eliminated Dsh protein. Although embryos with reduced levels of Dsh protein (67% of control levels) develop normally, it is not possible to deduce from this whether Dsh is required for regulating the specification of the dorsal axis (Heasman, J., J.R. Miller, and R.T. Moon, unpublished observations). Therefore, the development of dorsal cell fates in oligo-depleted embryos can be explained by the perdurance of Dsh protein. Thus, demonstrating a requirement for Dsh function in dorsal development must await new loss-of-function methods for examining gene function in *Xenopus*.

We thank Dr. Karl Willert and Dr. Roel Nusse for providing anti-mouse Dvl-1 antibodies before publication. We thank Mike Wu for assistance with oocyte injection experiments. We thank Dr. Janet Heasman for providing unpublished results and Dsh oligonucleotide-depleted embryos for Western blot analyses. The authors give special thanks to Dr. John Gerhart for valuable discussions.

This research was supported by National Institutes of Health grant HD29360 (R.T. Moon). C.A. Larabell is supported by the Department of Defense/Breast Cancer Research Program (grant B696-337). J.R. Miller is supported as an Associate, and R.T. Moon as an Investigator, of the Howard Hughes Medical Institute.

Submitted: 27 January 1999

Revised: 14 June 1999

Accepted: 17 June 1999

## References

- Aberle, H., A. Bauer, J. Stappert, A. Kispert, and R. Kemler. 1997.  $\beta$ -catenin is a target for the ubiquitin-proteasome pathway. *EMBO (Eur. Mol. Biol. Organ.) J.* 16:3797–3804.
- Axelrod, J.D., K. Matsuno, S. Artavanis-Tsakonas, and N. Perrimon. 1996. Interaction between Wingless and Notch signaling pathways mediated by Dishevelled. *Science*. 271:1826–1832.
- Axelrod, J.D., J.R. Miller, J.M. Shulman, R.T. Moon, and N. Perrimon. 1998. Differential recruitment of Dishevelled provides signaling specificity in the planar cell polarity and Wingless signaling pathways. *Genes Dev.* 12:2610–2622.
- Brannon, M., M. Gomperts, L. Sumoy, R.T. Moon, and D. Kimelman. 1997. A  $\beta$ -catenin/XTcf-3 complex binds to the *siamois* promoter to regulate dorsal axis specification in *Xenopus*. *Genes Dev.* 11:2359–2370.
- Brannon, M., J.D. Brown, R. Bates, D. Kimelman, and R.T. Moon. 1999. XTcfBP is a XTcf-3 co-repressor with roles throughout *Xenopus* development. *Development*. 126:3159–3170.
- Cadigan, K.M., and R. Nusse. 1997. Wnt signaling: a common theme in animal development. *Genes Dev.* 11:3286–3305.
- Elinson, R.P., and B. Rowning. 1988. A transient array of parallel microtubules in frog eggs: potential tracks for a cytoplasmic rotation that specifies the dorso-ventral axis. *Dev. Biol.* 128:185–197.
- Giebelhaus, D.H., B.D. Zelus, S.K. Henchman, and R.T. Moon. 1987. Changes in the expression of a-fodrin during embryonic development of *Xenopus laevis*. *J. Cell Biol.* 105:843–853.
- Harland, R., and J.C. Gerhart. 1998. Formation and function of Spemann's Organizer. *Annu. Rev. Cell Dev. Biol.* 13:611–667.
- Heasman, J., A. Crawford, K. Goldstone, P. Garnerhamrick, B. Gumbiner, P. McCrea, C. Kintner, C.Y. Noro, and C. Wylie. 1994. Overexpression of cadherins and underexpression of  $\beta$ -catenin inhibit dorsal mesoderm induction in early *Xenopus* embryos. *Cell*. 79:791–803.
- Holowacz, T., and R.P. Elinson. 1993. Cortical cytoplasm, which induces dorsal axis formation in *Xenopus*, is inactivated by UV irradiation of the oocyte. *Development*. 119:277–285.
- Hoppler, S., J.D. Brown, and R.T. Moon. 1996. Expression of a dominant-negative Wnt blocks induction of MyoD in *Xenopus* embryos. *Genes Dev.* 10:2805–2817.
- Kageura, H. 1997. Activation of dorsal development by contact between the cortical dorsal determinant and the equatorial core cytoplasm in eggs of *Xenopus laevis*. *Development*. 124:1543–1551.
- Larabell, C.A., B.A. Rowning, J. Wells, M. Wu, and J.C. Gerhart. 1996. Confocal microscopy analysis of living *Xenopus* eggs and the mechanism of cortical rotation. *Development*. 122:1281–1289.
- Larabell, C.A., M. Torres, B.A. Rowning, C. Yost, J.R. Miller, M. Wu, D. Kimelman, and R.T. Moon. 1997. Establishment of the dorso-ventral axis in *Xenopus* embryos is presaged by early asymmetries in  $\beta$ -catenin that are modulated by the Wnt signaling pathway. *J. Cell Biol.* 136:1123–1136.
- Laurent, M.N., I.L. Blitz, C. Hashimoto, U. Rothbacher, and K.W. Cho. 1997. The *Xenopus* homeobox gene *twin* mediates Wnt induction of *gooseoid* in establishment of Spemann's organizer. *Development*. 124:4905–4916.
- McKendry, R., S.C. Hsu, R.M. Harland, and R. Grosschedl. 1997. LEF-1/TCF proteins mediate Wnt-inducible transcription from the *Xenopus nodal-related 3* promoter. *Dev. Biol.* 192:420–431.
- McMahon, A., and R.T. Moon. 1989. Ectopic expression of the proto-oncogene *int-1* in *Xenopus* embryos leads to duplication of the embryonic axis. *Cell*. 58:1075–1084.
- Miller, J.R., and R.T. Moon. 1996. Signal transduction through  $\beta$ -catenin and specification of cell fate during embryogenesis. *Genes Dev.* 10:2527–2539.
- Miller, J.R., and R.T. Moon. 1997. Analysis of the signaling activities of localization mutants of  $\beta$ -catenin during axis specification in *Xenopus*. *J. Cell Biol.* 139:229–244.
- Molenaar, M., M. van de Wetering, M. Oosterwegel, J. Peterson Maduro, S. Godsave, V. Korinek, J. Roose, O. Destree, and H. Clevers. 1996. XTcf-3 transcription factor mediates  $\beta$ -catenin-induced axis formation in *Xenopus* embryos. *Cell*. 86:391–399.
- Moon, R.T., and D. Kimelman. 1998. From cortical rotation to organizer gene expression: toward a molecular explanation of axis specification in *Xenopus*. *Bioessays*. 20:536–545.
- Nordermeier, J., J. Klingensmith, N. Perrimon, and R. Nusse. 1994. *dishevelled* and *armadillo* act in the *wingless* signaling pathway in *Drosophila*. *Nature*. 367:80–83.
- Orford, K., C. Crockett, J.P. Jensen, A.M. Weissman, and S.W. Byers. 1997. Serine phosphorylation-regulated ubiquitination and degradation of  $\beta$ -catenin. *J. Biol. Chem.* 272:24735–24738.
- Roose, J., M. Molenaar, J. Peterson, J. Hurenkamp, H. Brantjes, P. Moerer, M. van de Wetering, O. Destree, and H. Clevers. 1998. The *Xenopus* Wnt effector XTcf-3 interacts with Groucho-related transcriptional repressors. *Nature*. 395:608–612.
- Rowning, B.A., J. Wells, M. Wu, J.C. Gerhart, R.T. Moon, and C.A. Larabell. 1997. Microtubule-mediated transport of organelles and localization of  $\beta$ -catenin to the future dorsal side of *Xenopus* eggs. *Proc. Natl. Acad. Sci. USA*. 94:1224–1229.
- Scharf, S.R., B. Rowning, M. Wu, and J.C. Gerhart. 1989. Hyperdorsoanterior embryos from *Xenopus* eggs treated with  $D_2O$ . *Dev. Biol.* 134:175–188.
- Schneider, S., H. Steinbeisser, R.M. Warga, and P. Hausen. 1996.  $\beta$ -catenin translocation into nuclei demarcates the dorsalizing centers of frog and fish embryos. *Mech. Dev.* 57:191–198.
- Sokol, S.Y., J. Klingensmith, N. Perrimon, and K. Itoh. 1995. Dorsalizing and neuralizing properties of Xdsh, a maternally expressed *Xenopus* homolog of *dishevelled*. *Development*. 121:1637–1647.
- Sokol, S.Y. 1996. Analysis of Dishevelled signaling pathways during *Xenopus* development. *Curr. Biol.* 6:1456–1467.
- Yanagawa, S., F. van Leeuwen, A. Wodarz, J. Klingensmith, and R. Nusse. 1995. The Dishevelled protein is modified by wingless signaling in *Drosophila*. *Genes Dev.* 9:1087–1097.
- Yang-Snyder, J., J.R. Miller, J.D. Brown, C.J. Lai, and R.T. Moon. 1996. A frizzled homolog functions in a vertebrate Wnt signaling pathway. *Curr Biol.* 6:1302–1306.
- Yost, C., M. Torres, J.R. Miller, E. Huang, D. Kimelman, and R.T. Moon. 1996. The axis-inducing activity, stability, and subcellular distribution of  $\beta$ -catenin is regulated in *Xenopus* embryos by glycogen synthase kinase 3. *Genes Dev.* 10:1443–1454.
- Yost, C., G.H.R. Farr, S.B. Pierce, D.M. Ferkey, M.M. Chen, and D. Kimelman. 1998. GBP, an inhibitor of GSK-3, is implicated in *Xenopus* development and oncogenesis. *Cell*. 93:1031–1041.
- Zeng, L., F. Fagotto, T. Zhang, W. Hsu, T.J. Vasicek, W.L. Perry, J.J. Lee, S.M. Tilghman, B.M. Gumbiner, and F. Costantini. 1997. The mouse *fused* locus encodes Axin, an inhibitor of the Wnt signaling pathway that regulates embryonic axis formation. *Cell*. 90:181–192.